Combining observations for re-entry purposes

Benjamin Bastida Virgili
IMS Space Consultancy @ ESA Space Debris Office, ESOC/ESA
Stijn Lemmens
ESA Space Debris Office, ESOC/ESA
Jan Siminski
IMS Space Consultancy @ ESA Space Debris Office, ESOC/ESA
Quirin Funke
IMS Space Consultancy @ ESA Space Debris Office, ESOC/ESA
Tim Flohrer
ESA Space Debris Office, ESOC/ESA

ABSTRACT

On average, two small tracked debris objects re-enter the Earth's atmosphere every day and burn up. Only a few very large objects, such as heavy science satellites, re-enter Earth's atmosphere in a year, while objects of moderate size, i.e. 1 m or larger, re-enter about once a week. Pieces of these large space debris objects (such as satellites, spent rocket bodies and large fragments) that re-enter the atmosphere in an uncontrolled way can reach the ground and pose a risk to the population or on-ground infrastructure. The related risk for an individual is, however, several orders of magnitude smaller than commonly accepted risks in daily life. The European Space Agency (ESA) Space Debris Office (SDO) provides information on upcoming and past re-entries to a wide target audience, including national civil protection agencies, researchers and the general public, via a web-based portal [1]. ESA also participates in and hosts a re-entry data exchange platform for the IADC (Inter-Agency Space Debris Coordination Committee).
In order to generate predictions for a given re-entry, orbital data of the object is required. There may be many different sources of data, provided in diverse formats like TLEs (two-line elements), orbital state vectors, or ephemeris, and sometimes raw data from various type of sensors. In that case, an additional process is needed to process the data and compute an orbit determination (OD), with a possible combination of data from different sources. The results of the data fusion are then used to increase the accuracy of the re-entry prediction results. Currently, ESA's main objective is to further automate the re-entry prediction process, which currently requires some expert interaction to exploit its full capabilities, and to reduce the uncertainties associated to the predictions.
In this paper, we explain how the adopted re-entry prediction process works, how the orbital data is combined, and we show some real re-entry cases (as the upper stage for Vega-01 AVUM (Attitude & Vernier Upper Module), the GOCE (Gravity Field and Steady-State Ocean Circulation Explorer) satellite, or the Tiangong-1 space station) where the method has been applied. In order to assess the prediction quality, we compare the prediction results using different combinations of orbital data between them, using as reference the final estimated re-entry time as provided by space-track.org or by observations from ground.

1. INTRODUCTION

The European Space Agency (ESA) has been hosting technical workshops on re-entries since the early 80's, as ESA provides a re-entry service to ESA's member states and also assumes the responsibility of a launching state for ESA-registered objects. The Space Debris Office (SDO) is tasked with the related development and research, and provides a re-entry service to registered users. In addition, ESA, as member of Inter-Agency Space Debris Coordination Committee (IADC), coordinates the re-entry campaigns of IADC, including campaign administration, web-based front-end hosting and maintenance.

An automated re-entry prediction process was set at ESA in 1999, with the LASCO (Lifetime Assessment for Catalogued Objects) [2] tool, which computes in a fully automated way the remaining lifetime for all objects in the public TLE catalogue and generates re-entry predictions. The results have been accessible via the DISCOS (Database and Information System Characterizing Objects in Space) web interface [3]. Since 2013 the results of the LASCO analysis containing the re-entry predictions for the following two months are more proactively distributed via e-mail to stakeholders subject to registration. Shortly after, in 2014, a new tool was created, called RAPID, which automates

the use of existing expert tools that are used to generate more accurate predictions during the last month of a re-entry, and with the capability of additional report generation. The last step of this modernization was taken in 2016, with the setup of a two-tier web based data distribution [1] aimed at civil protection agencies, with some contribution for the general public as well as part of ESA's educational responsibility. A more detailed explanation of the capabilities of the tools can be found in [4].

In order to generate predictions for a given re-entry, orbital data of the re-entering object is required. Currently, most of the predictions are based on using only US TLEs. However, for some particularly interesting re-entries, or as part of an IADC test campaign exercises which are conducted once per year, other sources of data may become available. In these cases, data is provided in diverse formats like TLEs (from a different originator than the US), orbital state vectors or even ephemeris, and sometimes also raw data from various type of sensors. If raw observation data is available, an additional process is needed to process it and to compute an orbit determination, with a possible combination of data from different sensors. The use of all sources of data can help increase the accuracy of the re-entry predictions, with a possible reduction of the uncertainty window. However, this is not always guaranteed, as combining the data may produce noisier results and an expert assessment is required to detect and correct such cases. Therefore, this processing using data from different sources is currently performed manually. ESA's objective is to automate the complete re-entry prediction process also for the complex cases in order to have a faster and more reliable prediction with reduced risk of manual errors.

In this paper, we first explain in some detail the re-entry prediction process at ESA. Then, we show the process to generate an orbit from observation data from different sources, which may be combined. Finally, we show some real re-entry cases for which IADC tests campaigns were performed and where more data was available and where the methods here presented have been applied (as the upper stage for Vega-01 AVUM, the GOCE satellite, and the Tiangong-1 space station). In order to assess the quality, we compare the prediction results using different combinations of orbital data between them, using as reference the final estimated re-entry time as provided by space-track.org, using the same statistical analysis as presented in [5, 6].

2. RE-ENTRY PROCESS

The routine automatic re-entry process at ESA uses daily updated orbital data, for example from the US TLE catalogue, to perform a ballistic coefficient estimation and a propagation from the last orbital state until re-entry. This is done by LASCO for all objects in the catalogue. In order to make a re-entry prediction, LASCO estimates the ballistic parameter (Bc) of the object by analyzing the orbital position history. Concretely, an iterative shooting method is applied to the orbital states within a time span where one searches the value of Bc such that the positional error while propagating from one observed orbital state to a consecutive one is minimized. A minimum time between two orbital states used for the shooting method is defined to limit the maximum amount of pairs. The mean value obtained for Bc is then used to propagate the object from the most recent state vector until re-entry, by means of different propagators which are selected depending on the time remaining until re-entry.
Once LASCO predicts that an object is re-entering in less than one month, a more accurate tool is automatically used, called RAPID. It uses first the ESA semi-analytical propagator called Fast Orbit Computation Utility Software (FOCUS) to fit the Bc analyzing the decrease of the semi-major axis of a set of TLE. Then, the orbit of the object is propagated from the last state until re-entry using an accurate numerical propagator called OrbGen. A quality criteria to decide whether a RAPID prediction is the root mean square (RMS) error obtained from the fitting of the drag coefficient on the semi-major axis (threshold at 10km) and on the position in orbit (threshold at 20 degrees). If the errors are above the threshold, the prediction using that particular set of data is considered unreliable. There are different reasons which trigger such large errors, such as wrong or inaccurate data, large gaps between data points, solar storms, orbit control maneuvers, etc. The expected uncertainty of the RAPID process is of 20% of the remaining orbital lifetime at the prediction epoch, which is considered the state-of-the art for re-entry predictions [7]. However, in practice the accuracy of the re-entry predictions performed with RAPID can be even as low as 5% under certain conditions [8], especially if a human intervention fixes the sources of errors. The shape of the uncertainty distribution is still subject to analysis, but postulated to be skewed normal when considering a few weeks to a few days of remaining orbital lifetime [9] to multimodal during the last orbital revolutions [10].

For the manual re-entry predictions, the RAPID tool is also used. The main difference with the automatic process is the possible additional orbital data from different originators and in different formats. This data is processed and

converted into TLE in order to be able to execute the RAPID ballistic coefficient calculation using the different inputs. The expert will then analyze the results of the processing, verify the estimated errors introduced for each of the different data points, and decide if the fit is correct or if some input has to be removed or corrected. In addition, the number of TLEs used for the Bc fitting is varied, in view of the past and predicted evolution of the solar activity, in order to compensate for extraordinary events such as geomagnetic storms which may not be properly reproduced by the atmosphere models. The predictions for the solar activity can also be varied, allowing to simulate storms and other events. Further, the state vector taken for the propagation (which usually is the most recent one), may also be varied. These variations can be done in an automated way via Monte-Carlo (MC) simulations, from which we are able to get a distribution with the most probable re-entry time, as can be seen in Fig. 1 for different atmosphere models. The expert running this time consuming process decides then on the best combination and produces a re-entry prediction. This work concentrates on the combination of observation data, however a large source of uncertainty for re-entries comes from the use of different atmosphere models [5,6].

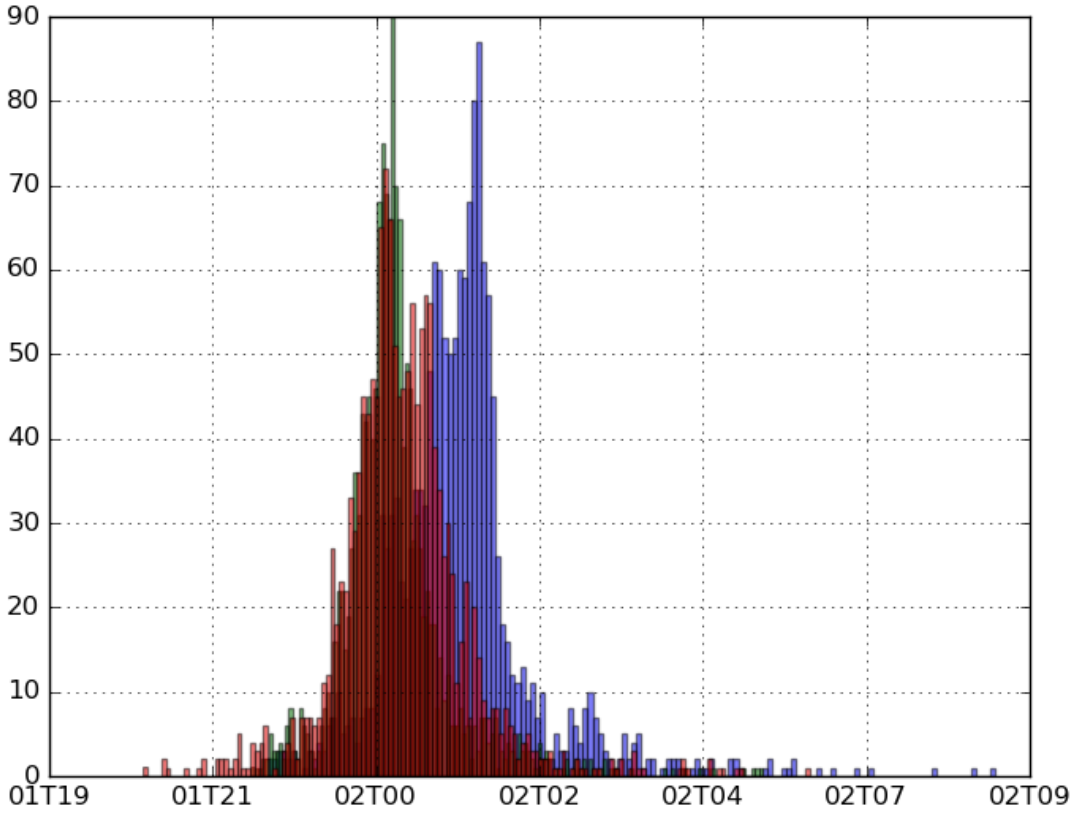

Fig. 1. Monte-Carlo distribution of re-entry times for Tiangong-1 based on data of 1st of April, with 3 different atmosphere models (DTM-13 in blue, NRLMSIS-00 in green and GOST-04 in red).

3. ORBIT DETERMINATION FROM DIFFERENT SOURCES OF DATA

There may be many different sources of data to be used for performing re-entry predictions, provided in different formats like TLEs, orbital state vectors, or ephemeris, and even sometimes also raw data from very different sensors. In that case, an additional data preparation process is needed to compute an orbit determination, which becomes more difficult in the last hours of a re-entry, causing the last inputs to the prediction process to be noisy. For the re-entry campaigns performed under IADC, campaign participants receive TLEs from international partners through the IADC exchange website for re-entry campaigns. For some specific re-entries ESA procured or obtained access to radar tracks (from TIRA and Santorcaz (ESA SSA)), radar range measurements (from EISCAT), SLR (satellite laser ranging) range data (from the Shanghai Astronomical Observatory) and optical observations (from the Mini-MegaTORTORA (MMT) observatory). In some cases, it is necessary to manually filter for outliers. In other cases, when data seems to be noisy but can be used, it is possible to perform a combination of noisy data in order to derive a mean state with less noise by fitting the data points to a new orbit.

3.1 Sources of data

3.1.1 TIRA

The TIRA (Tracking and Imaging Radar) radar is part of the Fraunhofer Research Establishment FHR - the Fraunhofer-Institut für Hochfrequenzphysik und Radartechnik (High Frequency Physics and Radar Techniques). TIRA is located at the FGAN site, in Wachtberg near Bonn, Germany, shown in Fig. 2. It consists of a tracking radar, working in L-Band (1.333 GHz), which also has imaging capabilities in Ku-Band (16.7GHz) that can be used to estimate the attitude of a re-entering object and help improve the drag coefficient (Cd) estimation. ESA collaborates with FHR to acquire TIRA passes to support re-entry predictions, improve the orbital information for chaser objects in case of close conjunctions, as well as for attitude analysis of debris, beam-park experiments and other research studies.

Fig. 2. FHR/TIRA radar.

3.1.2 Santorcaz radar

The monostatic breadboard surveillance radar was developed under ESA's SSA (Space Situational Awareness) Programme between 2010 and 2013. It is installed at the Santorcaz Naval Radio Communication Station, near Madrid. The radar is a phased array system, with 64 transmitter elements and 128 receiver elements. The transmitted signal is pulsed, using linear frequency modulation (LFM) in L-band. The system is currently on loan to the Spanish Ministry of Defense, but ESA can use it for dedicated measurement campaigns after prior agreement on the duration and scope.

3.1.3 EISCAT

EISCAT (European Incoherent SCATter Scientific Association) is an international scientific association with member institutes in several countries [11]. It conducts ionospheric and atmospheric measurements with radars. It operates in three countries: Finland, Norway and Sweden, and all facilities are located north of the Arctic Circle. Although they have a swamped scientific schedule, they may be able to schedule observations with brief notice time for satellites of interest, in agreement with ESA through the SSA program. Even without having tracking capabilities, the EISCAT radar in Tromsoe (see Fig. 3) is able to acquire passes with very short arcs (3 to 5 seconds) for re-entering objects which are visible from their high latitude, as was the case for the Vega-01 AVUM.

Fig. 3. EISCAT radar in Tromsoe.

3.1.4 SLR

Satellite Laser Ranging (SLR) uses short-pulse lasers and state-of-the-art optical receivers and timing electronics to measure the two-way time of flight (and hence distance) from ground stations to retroreflector arrays on Earth orbiting satellites. Laser ranging activities are organized under the International Laser Ranging Service (ILRS) [12], which provides global satellite and lunar laser ranging data and their derived data products to support research in geodesy, geophysics, Lunar science, and fundamental constants. There is an increasing interest on tracking non-cooperative satellites (objects without retroreflectors) from the SLR stations, with some recent success. The SLR stations have also tried to observe re-entering objects in the last days before decay, with very few success, mainly due to visibility constraints, limits of the pass prediction accuracy, and weather conditions. However, for Tiangong-1, the Shanghai Astronomical Observatory SLR station, was able to get ranging data just a few days before re-entry.

3.1.5 MMT optical data

The Mini-MegaTORTORA (MMT) system is a novel multi-purpose wide-field monitoring instrument built for and owned by the Kazan Federal University, presently operated under an agreement between Kazan Federal University and Special Astrophysical Observatory, Russia. It includes a set of nine individual channels installed in pairs on five equatorial mounts. Every channel has a celostate mirror installed before the Canon EF85/1.2 objective for a rapid (faster than 1 second) adjusting of the objective direction in a limited range (approximately 10 degrees to any direction), see Fig. 4. In their public website [13], an open photometric database of satellites identified in their data stream is available for analysis, which includes satellites on the re-entry phases, as Tiangong-1. In addition to the magnitude, the data includes also the distance from the station to the object, which can be used for OD.

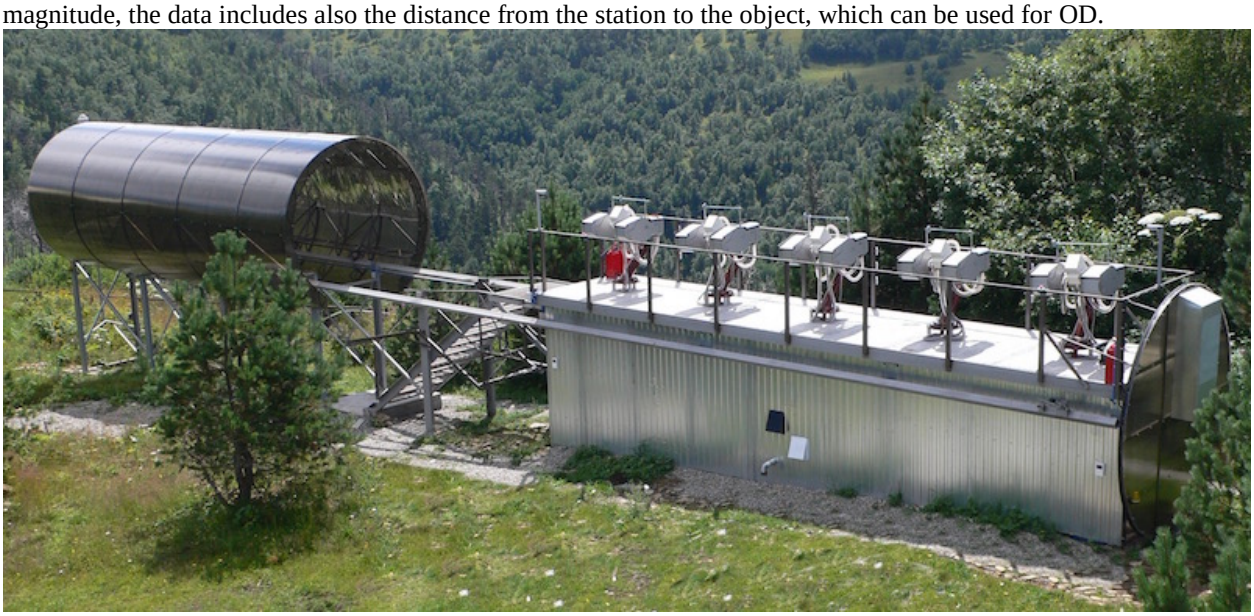

Fig. 4. MMT system.

3.2 Orbit determination

In order to perform an orbit determination based on the raw data received from the different sources, we use the tool ODIN (Orbit Determination by Improved Normal Equations) [14]. It implements the Levenberg-Marquardt batch least-squares technique to try to solve the OD problem. It is able to combine various available data, independently of the originator and the type of measurement taken, as only a pre-convertor is required to have the raw data in a similar format to be input to ODIN. There is no software limitation on the number of passes and stations that can be combined, although reaching convergence may become more difficult and time consuming when increasing the number, which is a general issue with fitting long-arcs at very low altitude.

In case of re-entries, an a-priori orbit is used to fit the measurements. For the last days of the re-entry this orbit needs to be close in time to the measurements, or the OD process may not converge to the right results. When this happens, manual iterations using different a-priori orbits (based on other available orbital date, like TLEs) are needed until a proper convergence is achieved. Having a single pass, from any source, usually allows to determine a converging orbit, but some of the orbital parameters may not be accurate enough and the drag coefficient cannot be properly estimated. In that case, it is possible to use the data by simulating another pass based on TLE data or on the a-priori orbit in order to improve the results. Once two or more passes are available, the results can be considered more reliable,

but this always depends on the geometry of the different passes, their duration and the time between them. Ideally, for a single station three passes separated by around 24h and in different pass directions give an optimal combination to perform a very precise OD, but with two passes and enough spacing it is also possible [15]. The option to use data from more than one sensor allows to have different pass geometries and a more frequent coverage of the objects, improving the quality of the OD results, which can be evaluated by assessing the residuals of the process. In case some residuals are unexpectedly large (much larger than the expected noise for any of the sensors), the results are considered erroneous and the OD is repeated in an iterative way. For the re-entry process, once the residuals are considered acceptable, the state vector at the OD epoch is converted in TLE format which serves as input to RAPID. There, the results from the fitting of the Bc allow to compare each of the SV against other TLEs and to evaluate how they fit together, deciding then if they can be used for the re-entry predictions or if there is a need for more iterations on the OD process. The schema in Fig. 5 displays in a simplified way how the complete processing chain works.

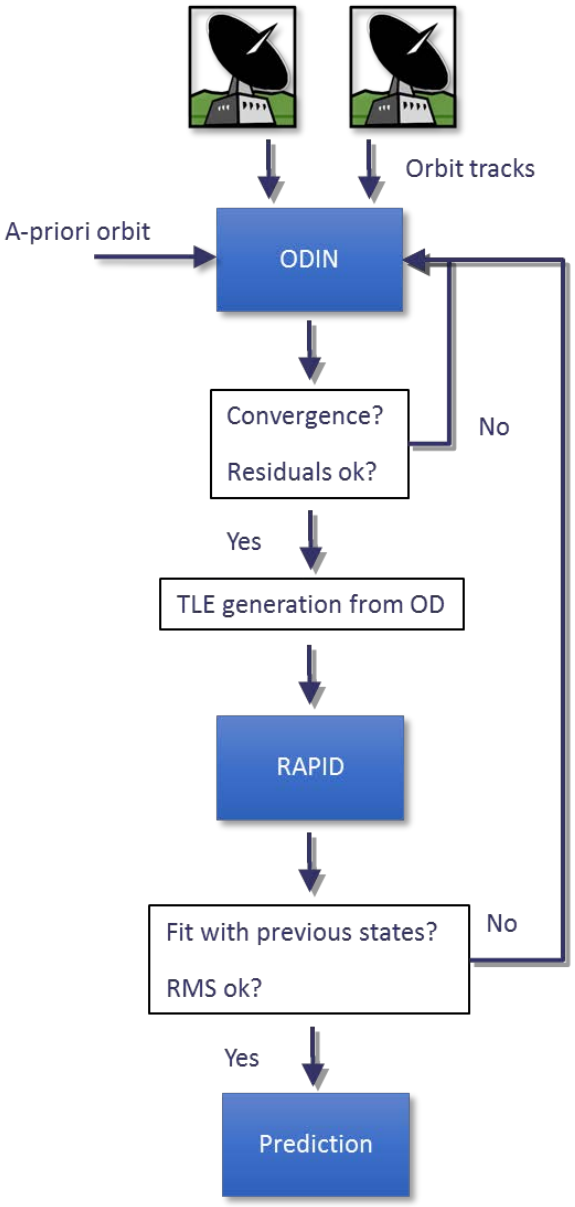

Fig. 5. OD and re-entry process chain

4. REAL RE-ENTRY CASES

There have been few selected cases in recent years where we were able to use raw data from different sources to derive a state vector which could be then used for re-entry predictions.

4.1 GOCE

ESA proposed to analyze GOCE's re-entry for the IADC test campaign of 2013, and the proposal was accepted [16]. The campaign opened on the 21st October 2013, after fuel depletion of the drag-compensating ion propulsion. GOCE was expected to enter into a phase of attitude-controlled fine-pointing mode (FPM), which would last approximately 2 weeks, until finally the attitude controllers would be unable to cope with the atmospheric torques. At that moment the satellite would enter in a phase of fully uncontrolled flight, which, due to deviations from the nominal attitude and the resulting increased cross section, would lead to an even faster decay and earlier re-entry. It happened, however, that a stable fine-pointing mode was maintained until the very final phase of the re-entry that kept GOCE in a head-on, minimum drag configuration, during the re-entry campaign. GOCE re-entered with the center of impact window on 11-Nov-2013 00:23 UTC.
As GOCE was controlled until the very last pass before re-entry, the flight dynamics (FD) team at ESOC (European Space Operation Center) was receiving data from the GPS receiver on board of the satellite. This data (see also [17]), in addition to the tracking data from the ground stations, allowed to determine a precise orbit during all the campaign, which could be used by the ESA SDO team, which is also located in ESOC. In addition, dedicated radar tracking was requested to TIRA [8], from which it was possible to compute orbits, which had comparable quality to the FD derived ones, and to derive the attitude of the satellite, which was in agreement to what the Flight Control Team was obtaining. The parallel IADC re-entry test campaign complemented the prediction, as this provided other sources for orbital data. All these available orbit information was processed in a combined way to generate the daily re-entry predictions, via the RAPID process and using TLEs, without the need to perform OD from different sources.

For this case, 12 TIRA passes were obtained, in groups of three passes at the beginning of the campaign, once every week (the azimuth, elevation and direction of the passes for the first week is displayed in Fig. 6), to enable good visibility geometries and improve OD performance. Then, during the last four days we retrieved 2 passes per day, allowing a continuous generation of an orbit (independently of other means), for the final phase of the re-entry. As GOCE was still controlled, it is clear that the data gathered during the re-entry down to altitudes slightly above 100km can help enormously to contribute to the validation of the simulators in different ways. From our point of interest, it has served as validation of the OD process on these very low altitudes, as well as to confirm which kind of geometries for the radar passes provide better results.

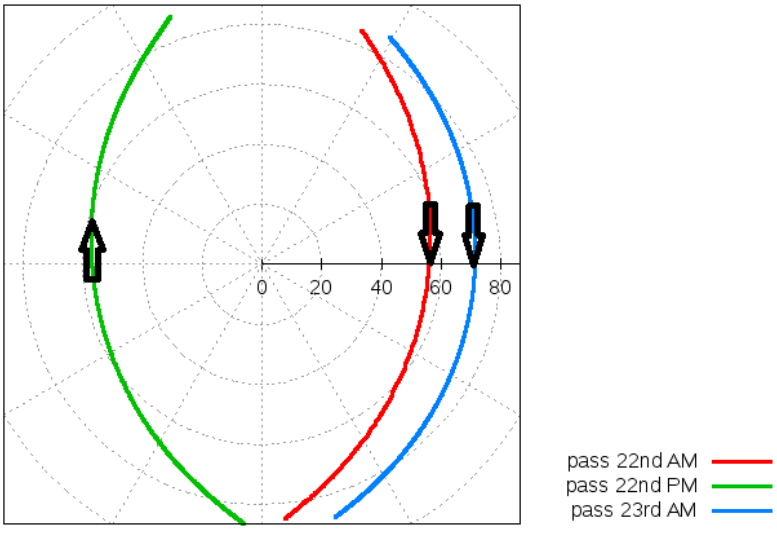

Fig. 6. Skyplot for the geometry of the passes acquired by TIRA on the 22nd and 23rd of October 2013 for GOCE

In Fig. 7 we can observe the apogee and perigee decay from the different orbital information at their generation epochs during the re-entry campaign, which are with a moderate orbit eccentricity of around 18km difference between apogee and perigee. Obviously, some points are very noisy and should have been filtered out by the process. However, we keep them in the plot to show the variability, and to point out that using them could cause a wrong prediction, as the fit and propagation from any of these noisy states would provide a completely different re-entry time.

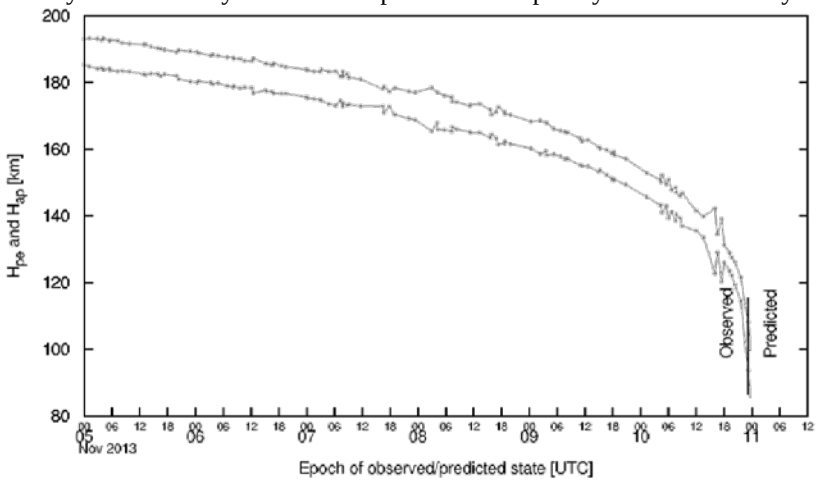

Fig. 7. Apogee and perigee altitude for GOCE of the different determined orbital states during the re-entry campaign.

4.2 Vega-1 AVUM

Since April 2016, when Vega-01 AVUM was selected as candidate for an IADC test campaign, the ESA SDO set up RAPID so that it would run the more precise predictions for the AVUM once per day, using for each prediction the most recent 20 US TLE available at that time [18]. The evolution of these fully automated predictions (including the uncertainty window) are shown in Fig. 8, where the large variations are mainly due to the uncertainty on the solar flux predictions. The IADC test campaign opened on the 18th October 2016, two weeks before the expected re-entry. This opening marked the start of a period of intense manual calibration work. For the AVUM campaign, we received TLEs from international partners through the IADC exchange website for re-entry campaigns, TIRA radar tracks, EISCAT range measurements and we tried to obtain SLR (satellite laser ranging) data from European stations, without success mainly due to bad meteorological conditions. The final re-entry was on the 2nd November 2016 at 4:49 UTC.

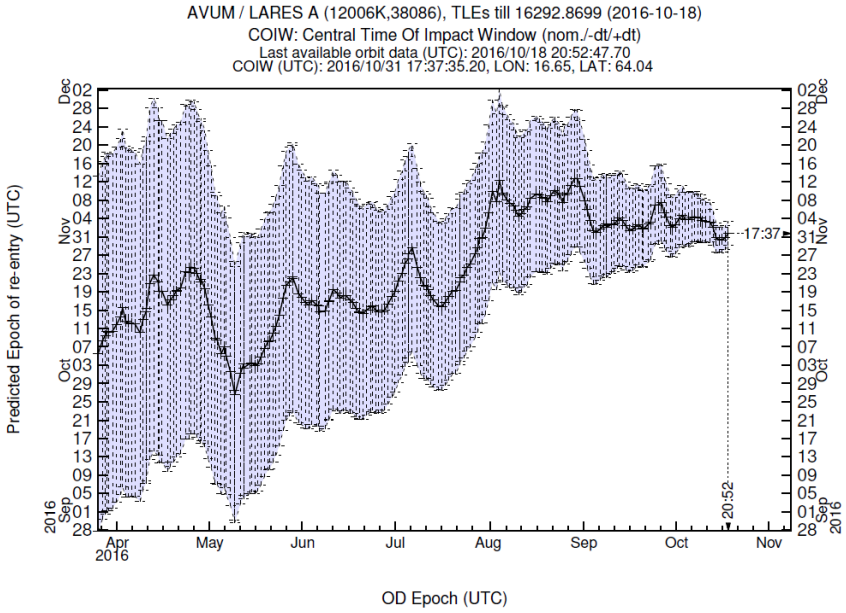

Fig. 8. Automated re-entry predictions for the AVUM since April 2016.

For detailed analysis of the AVUM we acquired three TIRA tracks, also with imaging to be able to determine the attitude of the object. The first one was on the 20th of October, the other two on the 27th and 28th of October. In between, we also received three EISCAT tracks, very short (3 to 5 seconds arc) but which could be used combined with the first TIRA track, and also as only source, on the 21st and 22nd of October. EISCAT also managed to acquire a track on the 1st of November (on the day before the re-entry), for which unfortunately the raw data arrived too late to be used for real-time predictions.
As shown for GOCE in Fig. 7, sometimes the TLEs used for the predictions are very noisy, especially when getting closer to the re-entry. This is mainly due to the difficulties that are encountered on the OD process, particularly if only one pass is used to fit the orbit, and it applies for any originator of TLEs. Therefore, for this campaign we used a filtering method to reduce this error: instead of using each TLE as direct input for the re-entry process, we use them as observation points to perform an OD. The result is a fitted orbit which is much less noisy. In Fig. 9, one can observe the many orbital states acquired during the campaign and how the noise is reduced compared to the case of GOCE thanks to this improvement.

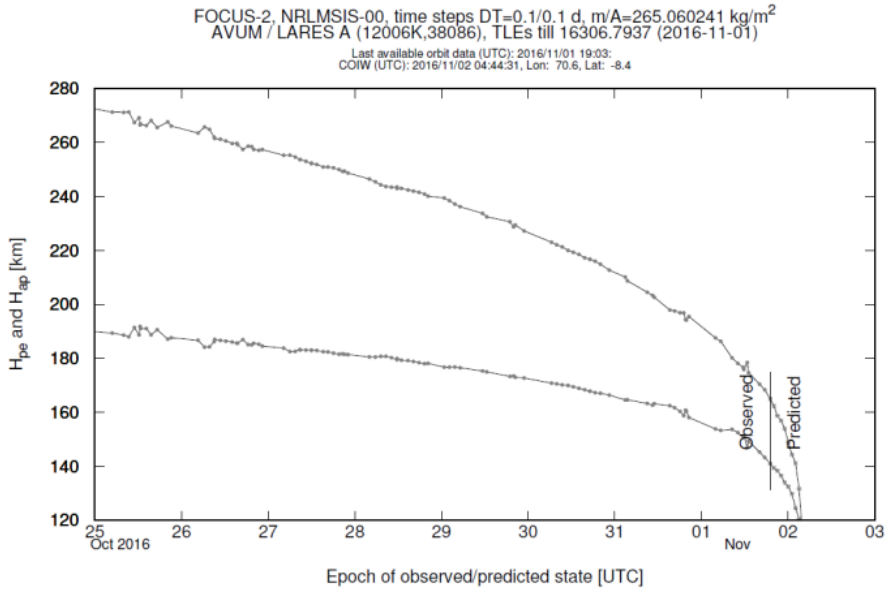

Fig. 9. Apogee and perigee evolution of the observed states, and prediction for the remaining time, for the AVUM re-entry.

4.3 Tiangong-1

The Tiangong-1 space station was selected as candidate for the 2018 test campaign in April 2017. The campaign started on the 12th February 2018, exceptionally early with more than one month to go until predicted re-entry (instead of the usual two weeks), with the expectation that more data could be shared through the IADC campaign between the participants in addition to TLEs. The main source of uncertainty during the campaign was the predicted solar activity, which compared to the observed one switched the prediction by almost 24 hours when only 3 days were remaining to re-entry. The final re-entry occurred on the 2nd of April 2018 at 00:16 UTC.

For this campaign, we obtained 14 TIRA radar passes of Tiangong-1, some with imaging in order to be able to derive the attitude motion of the space station. Two of them were obtained one week before the expected re-entry, while the rest were acquired daily since the 26th of March (and with 2 or 3 passes per day on the last 3 days). This enabled a continuous capability to generate reliable ODs. SLR observations from Europe suffered from poor visibility conditions. In addition, ESA's Santorcaz radar data was made available to ESA by the Spanish SST project of CDTI (Center for the Development of Industrial Technology, Spain) for post-analysis of the event, under the scope of the loan agreement between the Spanish Ministry of Defense and ESA. The campaigns for obtaining the data were funded by the 1SST2016_17 Grant Agreement with the European Commission (237/G/GRO/COPE/16/8935).
Post-event analysis using the Santorcaz data was possible, using 10 acquired passes for the last week before re-entry from Santorcaz, with one pass per day on the last few days, and two passes on the first days. A SLR station in Shanghai was also able to get a pass on the last day before re-entry, and shared the information with ESA a-posteriori.

Furthermore, also after the decay, we could obtain data from the MMT optical sensor which had observed Tiangong-1 on the 1st of April. All this new information in addition to the TIRA passes, concentrated on the last days before the re-entry, has been used to put in practice the combination of raw data to improve the OD process.
In Fig. 10 we show the six passes which have been used to test this combination of data. It is important to point out that, as Tiangong-1 had an orbital inclination of 42.7 degrees, the passes from TIRA had very low elevation, while the other stations had slightly better observation conditions. However, except for the Shanghai station, the rest have all similar pass geometries, with the same section of the orbit being observed. Their different locations is what provides an advantage in the OD. The orbit determination process converged with acceptable residuals only after excluding one pass. The result is consistent with the reference solution obtained in real-time with TIRA data only. We were also able to obtain convergence using different combinations of data, with one or more stations involved. Exemplary comparison of the orbit positions are shown in Fig. 11, where it is clear that the results of the OD are not exactly the same. This would bring the re-entry to a slightly different epoch. In real-time, our only way to check if an OD is correct is the comparison with previous states, for example in the plots with the evolution of perigee and apogee, as displayed in Fig. 12. A-posteriori, a similar approach can be used, and in addition a propagation starting from the computed state until re-entry allows to compare the re-entry epoch with the observed one. The comparison of such results with the ones of the real-time predictions, as well as with the observed re-entry time, are shown in Table 1. With this analysis, we always got a re-entry epoch which is closer to the real one than the real-time prediction done at a similar epoch. Part of the improvement may be due to the a-posteriori knowledge of the solar activity, but another part has to do with a better OD thanks to the use of multiple stations.

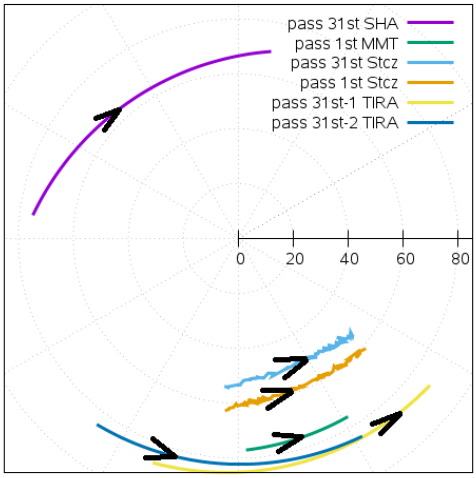

Fig. 10. Geometry of the passes acquired by different station on the 31st of March and 1st of April for Tiangong-1.

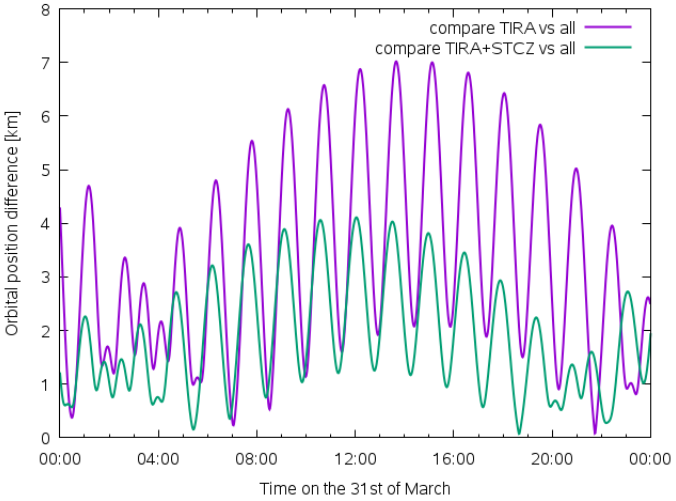

Fig. 11. Comparison on the 31st of March of the OD position for various cases. “TIRA” account for the results obtained in the real-time prediction, “TIRA+STCZ” adds the 2 Santorcaz tracks to the 2 TIRA tracks, and “all” considers using the 5 different tracks from the combination of data for the 4 stations.

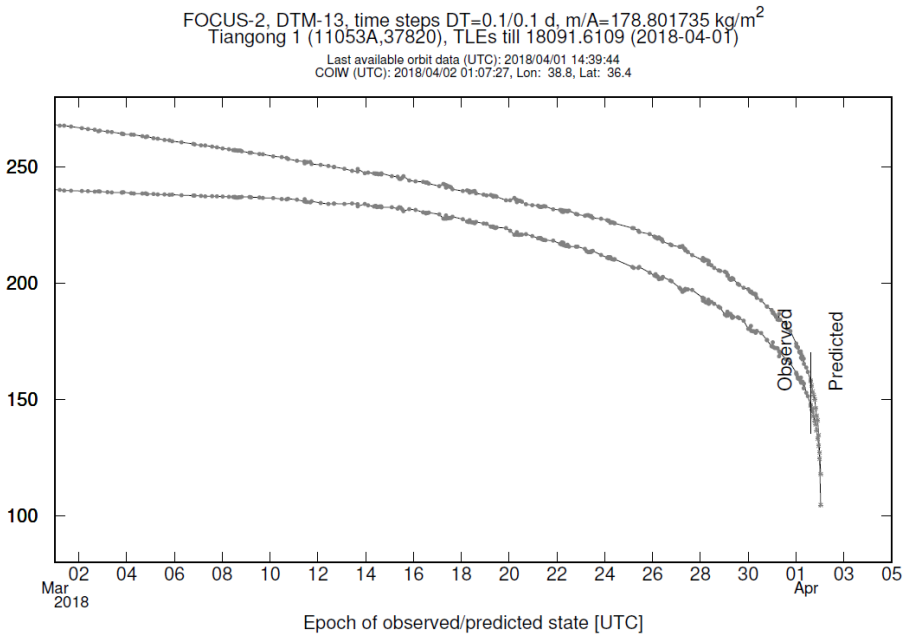

Fig. 12 Apogee and perigee evolution of the observed states, and prediction for the remaining time, for the Tiangong-1 re-entry.

Table 1. Event prediction consistency. Real observed re-entry time was 2018-04-02 00:16

Type of prediction	Time of last SV used for prediction	Predicted re-entry time
Real-time	2018-03-31 06:54	2018-04-01 23:25
2 TIRA + 2 STCZ tracks	2018-03-31 06:54	2018-04-02 00:05
Real-time	2018-04-01 06:19	2018-04-02 01:27
All (TIRA, STCZ, SHA2, MMT)	2018-04-01 06:54	2018-04-02 00:46

Comparing the re-entry epoch is however not the best solution to evaluate the advantages provided by the availability of extra stations. In order to better proof those, we have tested a different approach. For this, we consider that only TIRA radar passes are available, excluding also external orbital states. This means that to perform an OD with the first pass of a day the a-priori orbit is the one generated the day before. Due to the Tiangong-1 orbit, the separation between passes on consecutive days is around 20 hours. This procedure works fine if an object is at high altitude, but once you get to very low altitudes on the 2-3 days before a re-entry, obtaining an acceptable OD gets more difficult. If then another station would provide a pass which is in between the visibility gaps for TIRA, an update would be possible and then the convergence to an acceptable OD is easier. This can be illustrated with the TIRA passes on the 31st of March (5:20 and 6:50 UTC) and 1st of April (04:45, 06:15 and 07:47 UTC), where in real-time, to get a proper convergence of the passes for the 1st of April we needed an a-priori orbit based on a TLE from the early morning of the 1st of April. If we used instead as a-priori the orbit generated with the passes on the 31st, the results converged to an orbit which made no sense. If then we add the Shanghai pass on the 31st of March at 19:53 UTC to do an OD with the 2 TIRA passes on the 31st, the resulting orbit can be used as a-priori for the OD using the TIRA passes on the 1st of April, giving results very close to the ones obtained in real-time. There is a clear advantage, as that would allow a continuous capability to do re-entry predictions without need of other external data.

5. CONCLUSIONS

Re-entries of space debris occur on daily basis, with some of them being large enough so that some pieces reach ground. For those, sometimes internationally coordinated re-entry test campaigns are conducted under IADC, while most of them happen without any special follow-up. ESA shares information on upcoming events via a dedicated web-based front-end. To feed this exchange, ESA has developed a robust automatic re-entry process, which relies on having a source of constant information of orbits, e.g. as provided by the US TLE catalogue.

We have shown that if alternative extra sources of data are available, either raw data from stations or already processed and provided as TLE, ESA is able to combine them and use them in the re-entry process, with an improvement of the results. However, this involves still a largely manual process as it only happens on particular cases.

The availability of dedicated sensors able to acquire data for re-entering objects and the sharing of the acquired data will reduce uncertainties on predictions. This process would allow to increase prediction quality for re-entries and to limit risk to on-ground infrastructure and population.

6. AKNOWLEDGMENTS

The authors want to acknowledge Zhang Zhongping (zzp@shao.ac.cn) for kindly providing and giving permission to use the data from the Shanghai Astronomical Observatory.

The authors also want to acknowledge Sergey Karpov for kindly giving permission to use the data from the Mini-MegaTORTORA system.

Finally, the authors also want to acknowledge the CDTI for kindly providing and giving permission to use the data from the Santorcaz radar.

7. REFERENCES

1. ESA's re-entry predictions. Online at: https://reentry.esoc.esa.int/
2. Bunte, K. D., Sdunnus, H., Mandeville, J.C., & Klinkrad, H. Ballistic Parameter and Lifetime Assessment for Catalogued Objects. *Proceedings of the 3th European Conference on Space Debris*, ESA, Darmstadt, Germany, 2001.
3. Flohrer, T., et al. DISCOS: Current Status and Further Developments. *Proceedings of the 6th European Conference on Space Debris*, ESA, Darmstadt, Germany, 2013.
4. Lemmens, S., Bastida Virgili, B. et al. From End-Of-Life To Impact On Ground: An Overview Of Esa's Tools And Techniques To Predicted Re-Entries From The Operational Orbit Down To The Earth's Surface. *Proceedings of the 6th ICATT*, ESA, Darmstadt, Germany, 2016.
5. Bastida Virgili, B., Lemmens, S. et al. Statistical comparison of ISO recommended thermosphere models and space weather proxy forecasting on re-entry predictions. *In 68th International Astronautical Congress*, Adelaide, Australia, September 2017.
6. Stevenson, E, Bastida Virgili, B. et al. Comparison of Atmosphere Models for Atmospheric Predictions. *In 4th International Space Debris Re-entry Workshop*, ESA, Darmstadt, Germany, 2018.
7. Klinkrad, H. Space Debris: Models and Risk Analysis, *Springer-Verlag*, United Kingdom, 2006.
8. Lemmens, S., Bastida Virgili, B. et al. Calibration of radar based re-entry predictions. *Proceedings of the 5th International GOCE User Workshop*, ESA, Paris, France, November 2014.
9. Minisci, E., Serra, R. et al. Uncertainty treatment in the GOCE re-entry. *Proceedings of the 1st IAA Conference on Space Situational Awareness (ICSSA)* Orlando, FL, USA. 2017.
10. Bacon. J. Minimum Dv For Targeted Spacecraft Disposal. *Proceedings of the 7th European Conference on Space Debris*, ESA, Darmstadt, Germany, 2017.
11. EISCAT scientific association. Online at: *https://www.eiscat.se/*
12. ILRS. Online at: *https://ilrs.cddis.eosdis.nasa.gov/*
13. MMT satellite data. Online at: *http://astroguard.ru/satellites*
14. Alarcón-Rodriguez, J. R., Klinkrad, H., Cuesta J. & Martinez, F. M. (2005). Independent Orbit Determination for Collision Avoidance. In *Proceedings of the 4th European Conference on Space Debris*. ESA SP-587.
15. Cicalo, S., Beck, J. et al. GOCE Radar-Based Orbit Determination For Re-Entry Predictions And Comparison With Gps-Based POD. *Proceedings of the 7th European Conference on Space Debris*, ESA, Darmstadt, Germany, 2017.

16. Bastida Virgili, B., Lemmens, S. et al. GOCE re-entry campaign. *Proceedings of the 5th International GOCE User Workshop*, ESA, Paris, France, November 2014.
17. Gini, F., Otten, M. et al. "Precise Orbit Determination for the GOCE Re-entry Phase. *Proceedings of the 5th International GOCE User Workshop*, ESA, Paris, France, November 2014.
18. Bastida Virgili, B., Lemmens, S. et al. . Practicalities of re-entry predictions – the VEGA-01 AVUM case. *In 7th European Conference on Space Debris*, Darmstadt, Germany, 2017.